



Dalton  
Transactions

**Synthesis, Structures and Catalytic Activity of Some BINOL  
Based Boronates and Boronium Salts**

Journal:	<i>Dalton Transactions</i>
Manuscript ID	DT-ART-03-2021-000842.R1
Article Type:	Paper
Date Submitted by the Author:	22-Mar-2021
Complete List of Authors:	Krepner, Clemens; Texas Tech University, Department of Chemistry and Biochemistry Garg, Shipra; Texas Tech University Unruh, Daniel; Texas Tech University, Chemistry and Biochemistry

SCHOLARONE™  
Manuscripts

## ARTICLE

## Synthesis, Structures and Catalytic Activity of Some BINOL Based Boronates and Boronium Salts

Shipra Garg, Daniel K. Unruh and Clemens Krempner\*

Received 00th January 20xx,  
Accepted 00th January 20xx

DOI: 10.1039/x0xx00000x

The BINOL supported chiral boronate ester [C<sub>10</sub>H<sub>12</sub>O<sub>2</sub>BC<sub>6</sub>F<sub>5</sub>(THF)] [(*R*)-**1**], [C<sub>10</sub>H<sub>12</sub>O<sub>2</sub>BC<sub>6</sub>F<sub>5</sub>(O=PEt<sub>3</sub>)] [(*R*)-**3**] and [C<sub>10</sub>H<sub>12</sub>O<sub>2</sub>BC<sub>6</sub>F<sub>5</sub>]<sub>2</sub> [(*R,R*)-**2**] as well as the chiral boronium salts [C<sub>10</sub>H<sub>12</sub>O<sub>2</sub>B(O=PEt<sub>3</sub>)<sub>2</sub>]<sup>+</sup>[B(O<sub>2</sub>C<sub>10</sub>H<sub>12</sub>)<sub>2</sub>]<sup>-</sup>, [(*R*)-**6**] and [C<sub>10</sub>H<sub>12</sub>O<sub>2</sub>B(O=SMe<sub>2</sub>)<sub>2</sub>]<sup>+</sup>[B(O<sub>2</sub>C<sub>10</sub>H<sub>12</sub>)<sub>2</sub>]<sup>-</sup> [(*R*)-**7**] have been synthesized, characterized by NMR spectroscopy, and the solid state structures of [(*R*)-**1**], [(*R,R*)-**2**] and [(*R*)-**3**] determined. Chiral ester [(*R*)-**1**] was found to be a potent Lewis acid, similar to B(C<sub>6</sub>F<sub>5</sub>)<sub>3</sub>, and capable of rapidly catalyzing the annulation of (*R*)-, (*S*)- and *rac*-styrene oxide with nitrene PhCH=N(O)Me to trans-2-methyl-3,6-diphenyl-1,4,2-dioxazine (trans-**11**) with high regio- and diastereoselectivities.

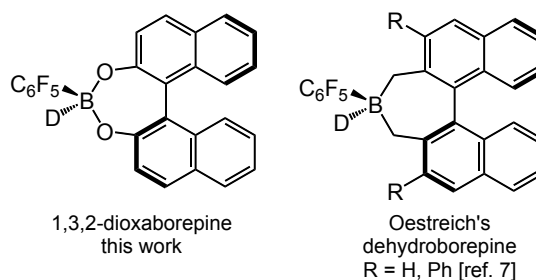
### Introduction

BINOL-substituted borates and boronates [1] represent a largely underdeveloped class of chiral boron compounds with interesting applications ranging from chiral sensing, quantitative analysis (Bull-James assembly) to dynamic covalent self-assembly [2]. In addition, they have found use as chiral Lewis acids catalysts in C-C bond forming reactions such as asymmetric allyl- and alkynylboration and Diels Alder reactions [3]. For example, Szabo et al. reported BINOL-catalysed asymmetric allyl-borations of ketones via in situ formed BINOL allyl boronates [4]. Ishihara and co-workers used in situ prepared BINOL based aryl boronates as catalysts for enantioselective Diels-Alder reactions of propargyl aldehydes and acrolein derivatives with dienes [5].

However, structurally well-characterized examples of trigonal planar boronates and borates are scarce [1a, 6], and while chiral anionic borates are well-documented, BINOL-substituted boronium and borenium cations are elusive species. In this regard, it should be noted that Oestreich and co-workers have disclosed the synthesis of chiral dehydroborepines with binaphtyl backbone and C<sub>6</sub>F<sub>5</sub> group at boron, which can be considered as carbon-based structural analogues of BINOL supported boronates (Scheme 1) [7]. These compounds proved to be promising catalysts in the Nazarov cyclization and enantioselective hydrosilylations of ketones and imines [8].

Inspired by these recent developments, we report herein the synthesis and structures of highly Lewis acidic BINOL-substituted pentafluorophenyl boronates and BINOL-supported boronium salts [9]. In addition, their catalytic activity in the

annulation of nitrene, PhCH=N(O)Me, with styrene oxide is described [10].



Scheme 1. Schematic presentation of chiral borepines with binaphtyl backbone.

### Results and Discussion

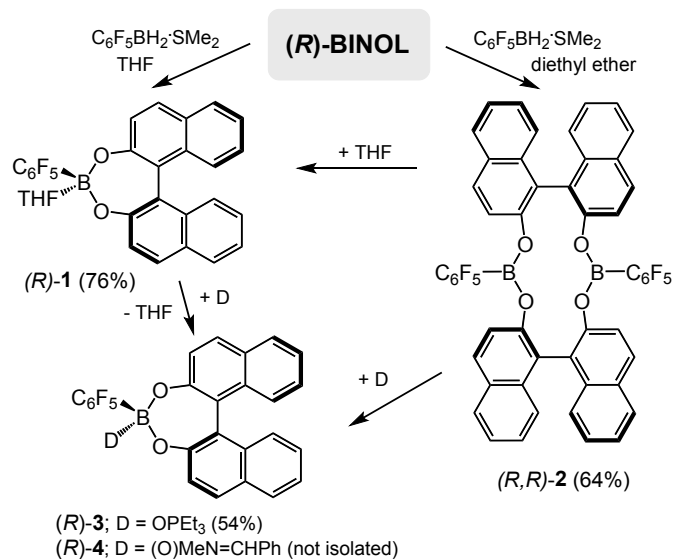
The synthesis of (*R*)-BINOL based boronates is illustrated in Scheme 2. Slow addition of a THF solution of (*R*)-BINOL to a THF solution of C<sub>6</sub>F<sub>5</sub>BH<sub>2</sub>·SMe<sub>2</sub> generates chiral boronate (*R*)-**1** in 76% yield. Compound (*R*)-**1** is a room temperature stable but very moisture sensitive crystalline material, which in addition to be analysed by NMR spectroscopy was structurally characterized by X-ray analysis (Figure 1). The X-ray data confirm the connectivity of the 1,3,2-dioxaborepin ring structure with a distorted tetrahedral geometry for boron via THF coordination. The B-O<sub>(THF)</sub> distance [1.597(8) Å] is significantly longer than the ring B-O distances with 1.451(7) and 1.418(8) Å, respectively. Notably, when the reaction was carried in diethyl ether, a crystalline material precipitated from solution, which by NMR spectroscopy and X-ray analysis (Figure 2) was identified as the binuclear boronate (*R,R*)-**2**. The data reveal trigonal planar geometry for both boron atoms and a 14-membered ring structure. The ring B-O distances range from 1.35 to 1.37 Å and are being significantly shorter than those of (*R*)-**1** with tetra-coordinated boron [1.451(7) and 1.418(8) Å]. Note that the twisting of the BINOL units is more pronounced in (*R,R*)-**2** with

<sup>a</sup> Department of Chemistry and Biochemistry, Texas Tech University, Memorial Dr. & Boston, Lubbock, TX, 79409, USA. Fax: 806-742-1289; Tel: 806-834-3507; E-mail: clemens.krempner@ttu.edu

<sup>†</sup> Footnotes relating to the title and/or authors should appear here.

Electronic Supplementary Information (ESI) available: [details of any supplementary information available should be included here]. See DOI: 10.1039/x0xx00000x

dihedral angles of 91 and 100° than in (*R*)-**1** with a dihedral angle of 49°.



**Scheme 2.** Reactions of  $\text{C}_6\text{F}_5\text{BH}_2\cdot\text{SMe}_2$  with (*R*)-BINOL.

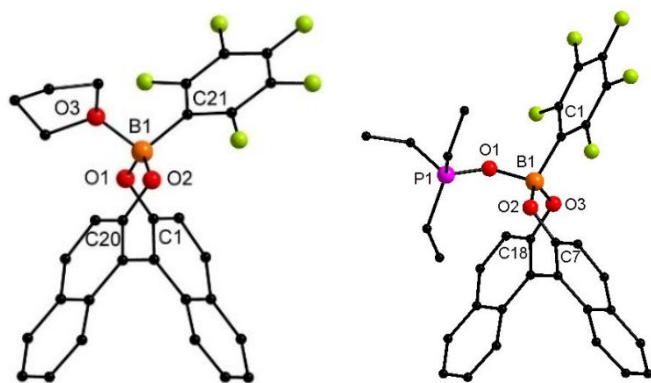


**Figure 1.** Solid-state structures of (*R*)-**1** (left) (H atoms and disordered THF omitted for clarity) and (*R*)-**3** (right) (H atoms omitted for clarity) (green = fluorine). Selected distances [Å] and angles [°]: (*R*)-**1**, C21 B1 1.632(5), O1 C1 1.370(4), O1 B1 1.444(5), O2 C20 1.379(4), O2 B1 1.425(5), O3 B1 1.601(5), O2 B1 O1 115.7(3), O2 B1 O3 109.4(3), O1 B1 O3 101.0(3); (*R*)-**3**, P1 O1 1.537(1), O1 B1 1.525(2), O2 C7 1.363(2), O2 B1 1.469(2), O3 C18 1.368(2), O3 B1 1.446(2), C1 B1 1.647(3), B1 O1 P1 133.4(1), O3 B1 O2 114.0(2), O3 B1 O1 109.1(2).

The results from the NMR spectroscopic analysis of both compounds in solution were consistent with the X-ray data. The <sup>11</sup>B NMR spectrum of (*R*)-**1** showed signals at around 8.8 (THF) and 13 ppm ( $\text{C}_6\text{D}_6$ ) suggesting tetra-coordination for boron, while (*R,R*)-**2** displayed one broad signal at around 30 ppm in  $\text{C}_6\text{D}_6$  confirming trigonal planar coordination environments for both boron atoms. The <sup>19</sup>F NMR spectra of (*R,R*)-**2** in  $\text{C}_6\text{D}_6$  showed one major set of three fluorine signals with an integral ratio of 2:1:2 indicating similar stereo-chemical environments for both  $\text{C}_6\text{F}_5$  groups. However, dissolving (*R,R*)-**2** in THF gives rise to signals in the <sup>11</sup>B and <sup>19</sup>F NMR spectra that are identical

to those of (*R*)-**1** confirming that (*R,R*)-**2** is readily converted to (*R*)-**1** in THF.

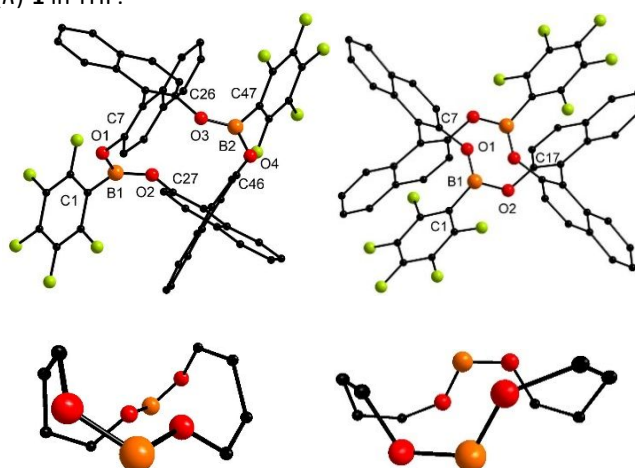
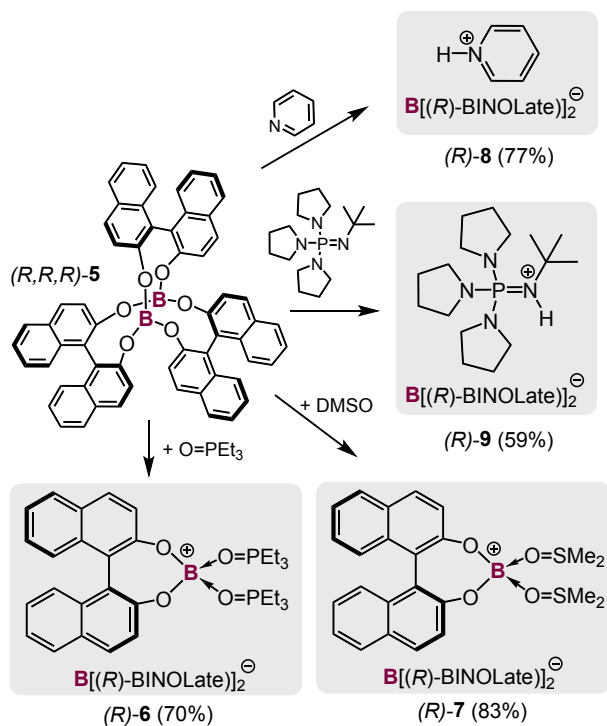


**Figure 2.** Top: Solid-state structures of (*R,R*)-**2** (left) and (*R,S*)-**2** (right). Hydrogen atoms omitted for clarity (green = fluorine); Bottom: Representation of the conformation of the 14-membered ring structures of (*R,R*)-**2** (left) and (*R,S*)-**2** (right). Selected distances [Å] and angles [°]: (*R,R*)-**2**, O1 B1 1.354(11), O1 C7 1.420(9), O2 B1 1.366(11), O2 C27 1.394(10), O3 B2 1.367(11), O3 C26 1.393(9), O4 B2 1.362(11), O4 C46 1.398(9), C1 B1 1.590(10), C47 B2 1.548(12), O1 B1 O2 117.8(8), O4 B2 O3 117.2(8); (*R,S*)-**2**, O1 B1 1.353(2), O1 C7 1.384(2), O2 B1 1.362(2), O2 C17 1.397(2), O1 B1 O2 116.7(1).

When (*rac*)-BINOL was treated with  $\text{C}_6\text{F}_5\text{BH}_2\cdot\text{SMe}_2$  in diethyl ether a crystalline precipitate was formed in good yields. While its <sup>11</sup>B NMR spectrum showed one signal at 8.5 ppm, the <sup>19</sup>F NMR spectrum revealed three sets of three signals each (1:1:1 ratio) suggesting the formation of a mixture of three stereoisomers of **2**, one of which was identified as (*R,R*)-**2** via <sup>19</sup>F NMR spectroscopy. A second stereoisomer could be identified by X-ray analysis as (*R,S*)-**2** (Figure 2). The data reveal trigonal planar geometry for both boron atoms and a 14-membered ring structure. While, the observed B-O and B-C distances and O-B-O angles are similar to those found in (*R,R*)-**2**, their ring conformations differ markedly with less BINOL twisting for (*R,S*)-**2** having a dihedral angle of 71°. Note that attempts to identify the third stereoisomer failed.

Next, (*R,R*)-**2** and (*R*)-**1** were reacted with O=PEt<sub>3</sub>, a strong donor frequently employed for Lewis acidity measurements or organo boranes via the classical Gutmann-Beckett method [11]. Thus, upon adding O=PEt<sub>3</sub> to  $\text{C}_6\text{D}_6$  solutions of (*R*)-**1** and (*R,R*)-**2**, resp., crystalline precipitates formed, which in both cases after isolation were identified by NMR spectroscopy and X-ray analysis as the thermally stable O=PEt<sub>3</sub> adduct (*R*)-**3** (54%). The X-ray data revealed strong donation of O=PEt<sub>3</sub> to the central boron giving rise to a B-O(O=PEt<sub>3</sub>) distance of 1.525(2) Å, which is significantly shorter than that of THF adduct (*R*)-**1** with a B-O<sub>THF</sub> distance of 1.597(8) Å. As a result, the B-O ring and B-C( $\text{C}_6\text{F}_5$ ) bond lengths of (*R*)-**3** are somewhat elongated (Figure 1). The <sup>31</sup>P NMR chemical shift of (*R*)-**3** was found to be at 76 ppm ( $\text{C}_6\text{D}_6$ ), which according to the following equation:  $\text{AN} = (\delta_{31\text{P}} - 41.0) \times (100 / (86.1 - 41.0))$ , corresponds to a Gutmann acceptor number (AN) of 77.4. This value is fairly similar to those found for other strong Lewis acids such as B( $\text{C}_6\text{F}_5$ )<sub>3</sub> (AN = 77.6) [12],  $\text{C}_6\text{F}_5\text{B-cat}$  (AN = 78.9) [13] and  $\text{C}_6\text{F}_5\text{B-nad}$  (AN = 80.9) [13].

We next investigated Kaufmann's bis-borate, (*R,R,R*)-**5** (Scheme 2) [1a], which is easily accessible in high purity from the reaction of R-BINOL with BH<sub>3</sub> in diethyl ether [see SI]. To estimate its Lewis acid strength, interactions with O=PEt<sub>3</sub> were studied through multi-nuclear NMR spectroscopy in C<sub>6</sub>D<sub>6</sub>. Notably, the <sup>31</sup>P NMR spectrum of the mixture displays a single signal at 82 ppm, which corresponds to an acceptor number of ca. 90.6, surprisingly high given that B(OC<sub>6</sub>F<sub>5</sub>)<sub>3</sub> has an acceptor number of only 88.4 [14]. We also noticed that two equiv. of O=PEt<sub>3</sub> were required to fully convert (*R,R,R*)-**5** to the new species (*R*)-**6**. Analysis by <sup>1</sup>H and <sup>13</sup>C NMR spectroscopy confirmed the presence of two molecules of O=PEt<sub>3</sub> per two chemically inequivalent BINOL moieties (1:2 integral ratio). The <sup>11</sup>B NMR spectrum exhibits two resonances at 2.1 and 8.3 ppm confirming two tetra-coordinated boron centres. Collectively, the NMR data of (*R*)-**6** appear to be consistent with the formulation as boronium *spiro*-borate [C<sub>10</sub>H<sub>12</sub>O<sub>2</sub>B(O=PEt<sub>3</sub>)<sub>2</sub>]<sup>+</sup>[B(O<sub>2</sub>C<sub>10</sub>H<sub>12</sub>)<sub>2</sub>]<sup>-</sup>, where two molecules of O=PEt<sub>3</sub> coordinate to the cationic boron centre (Scheme 3). To support this notion, attempts were made to the synthesis of structural analogues of (*R*)-**6**. While ketones did not react with (*R,R,R*)-**5**, addition of two equiv. of DMSO to a THF solution of (*R,R,R*)-**5** resulted in the rapid formation of a crystalline precipitate, which was identified by NMR spectroscopy as [C<sub>10</sub>H<sub>12</sub>O<sub>2</sub>B(O=SMe<sub>2</sub>)<sub>2</sub>]<sup>+</sup>[B(O<sub>2</sub>C<sub>10</sub>H<sub>12</sub>)<sub>2</sub>]<sup>-</sup>, [(*R*)-**7**]. Again, its <sup>11</sup>B NMR spectrum exhibits two resonances at 4.2 and 8.1 ppm, and the results from the integration of the aromatic versus the DMSO signals in the <sup>1</sup>H NMR spectrum agree with a ratio of two DMSO per two chemically inequivalent BINOL moieties (1:2 integral ratio). Unfortunately, attempts to confirm the connectivity of both boronium salts (*R*)-**6** and (*R*)-**7** by X-ray analysis failed due to the insufficient quality of the crystals.



**Scheme 3.** Reactions of Kaufmann's bis-borate (*R,R,R*)-**5** with various Lewis bases.

In an attempt to gain more structural information and expand the scope of this rearrangement reaction, various amines were treated with (*R,R,R*)-**5**. To our surprise, the outcome of these reactions was strikingly different. Thus, while the bulky amines 2,6-dimethyl pyridine and 2,2,6,6-tetramethylpiperidine (TMP) did not show any sign of a reaction with (*R,R,R*)-**5** in THF as solvent, pyridine slowly reacted over the course of several days to give a crystalline precipitate of pyridinium salt [pyrH]<sup>+</sup>[B(O<sub>2</sub>C<sub>10</sub>H<sub>12</sub>)<sub>2</sub>]<sup>-</sup> (*R*)-**8** in 77% yield. The reaction of (*R,R,R*)-**5** with one equiv. of the stronger phosphazene base, (pyrr)<sub>3</sub>P=NBU<sup>t</sup>, proceeded similarly to rapidly produce a crystalline precipitate of the phosphazanium salt [(pyrr)<sub>3</sub>P=NBU<sup>t</sup>]<sup>+</sup>[B(O<sub>2</sub>C<sub>10</sub>H<sub>12</sub>)<sub>2</sub>]<sup>-</sup> [(*R*)-**9**] in 59% yield. Both spirocyclic compounds were structurally fully characterized by multi nuclear NMR spectroscopy and the results of single crystal X-ray analyses (Figure 3). Contrary to the boronium salts (*R*)-**6** and (*R*)-**7**, which show two signals in <sup>11</sup>B NMR spectra, one signal was found for (*R*)-**8** [8.2 ppm] and (*R*)-**9** [8.2 ppm], respectively. While the <sup>1</sup>H NMR spectrum of (*R*)-**9** showed a doublet at 3.4 ppm (<sup>2</sup>J<sub>P-H</sub> = 10.7 Hz) clearly attributable to the NH-proton of the phosphazanium cation, the respective NH-proton of the pyridinium cation of (*R*)-**8** could not be detected. However, IR spectroscopic measurements confirmed the presence NH functionalities in both compounds.

We have not been able to clearly identify the proton source. Protonation of the base by hydrolysis, however, is unlikely as all reactions were carried out under strictly anhydrous conditions. Proton delivery by the solvent appears unlikely as well, since the reaction of (*R,R,R*)-**5** with (pyrr)<sub>3</sub>P=NBU<sup>t</sup> in C<sub>6</sub>D<sub>6</sub> did not lead to the deuterated form of phosphazanium salt (*R*)-**9** (see Figure S45).

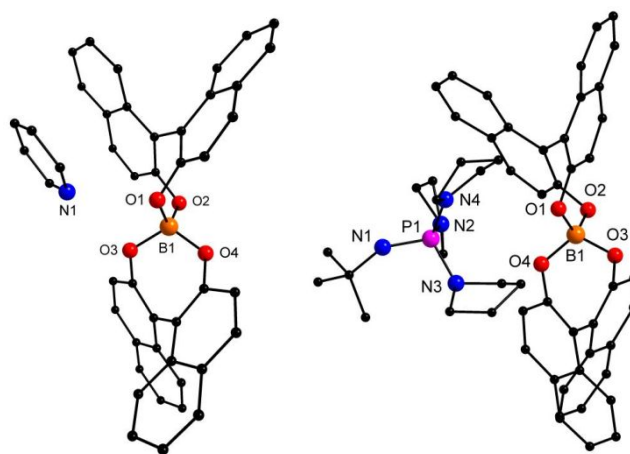


**Figure 3.** Solid-state structures of (*R*)-**8** (left) (for clarity, only one of the two independent molecules in the unit cell is shown, and all H atoms and co-crystallizing THF molecules are omitted) and (*R*)-**9** (right) (all H atoms omitted for clarity). Selected distances [Å] and angles [°]: (*R*)-**8**, O1 C2 1.358(3), O1 B1 1.472(3), O2 B1 1.467(3), O3 B1 1.490(3), O4 B1 1.457(3); (*R*)-**9**, O1 B1 1.469(3), O2 B1 1.475(3), O3 B1 1.460(3), O4 B1 1.471(3), P1 N1 1.635(2), P1 N2 1.624(2), P1 N3 1.641(2), P1 N4 1.633(2).

Given that only two of the BINOLate moieties of (*R,R,R*)-**5** are required to form (*R*)-**8** and (*R*)-**9**, respectively, it might be that boronium salts are involved as intermediates, which may serve as proton sources. This notion appears to be consistent with the observation that in the initial stage of the reaction of (*R,R,R*)-**5** with pyridine two boron signals at ca. 8.5 and 5.5 ppm are observed. The latter signal disappears and the former slightly shifts to higher field (ca. 8 ppm) over time as the formation of (*R*)-**8** progresses (see Figure S39).

When (*R,R,R*)-**5** was treated 1,3-dimesityl-imidazol-2-ylidene a mixture of products was formed with salt [1,3-dimesityl-imidazolium]<sup>+</sup>[B(O<sub>2</sub>C<sub>10</sub>H<sub>12</sub>)<sub>2</sub>]<sup>-</sup> as the dominant product, which could not be purified by crystallization. However, a few crystals suitable for X-ray analysis could be grown from the reaction mixture in benzene. The results are shown in Figure 4 and reveal the formation of (*R*)-**10**, a Lewis acid-base adduct derived from (*R,R,R*)-**5** and 1,3-dimesityl-imidazol-2-ylidene, that might be a potential intermediate in the formation of the corresponding boronium salts. As expected, the average B-O distances [1.36 Å] for boron with nearly trigonal planar coordination environment are significantly shorter than those of the tetra-coordinated boron with ca. 1.46 Å. The boron-carbene C1-B1 distance was found to be 1.709(4) Å, which is somewhat longer than those of the only two reported Lewis acid-base adducts with carbenes coordinating to B(OR)<sub>3</sub> moieties, namely, B<sub>2</sub>cat<sub>3</sub>-(<sup>i</sup>Pr<sub>2</sub>Im)<sub>2</sub> [1.652(4), 1.665(4) Å] [15] and RER-Dipp<sub>2</sub>Slm(H<sub>2</sub>)B-cat-Bcat-Dipp<sub>2</sub>Slm [1.663(7) Å] [16].

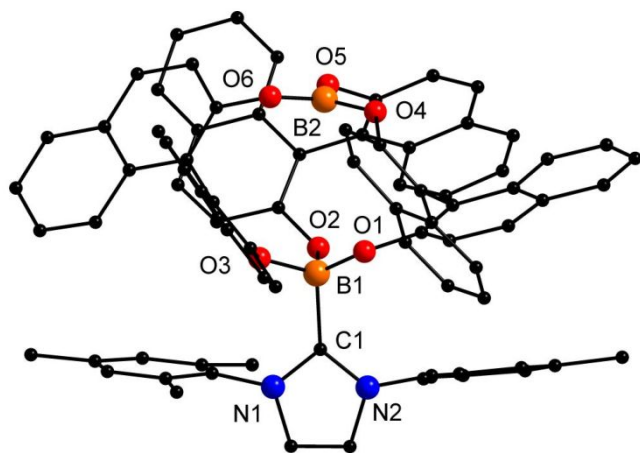
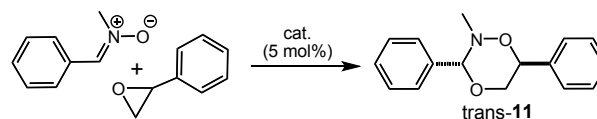


**Figure 4.** Solid-state structures of (*R*)-**10** (hydrogen atoms omitted for clarity). Selected distances [Å] and angles [°]: C1 B1 1.709(4), O1 B1 1.464(3), O2 B1 1.459(3), O3 B1 1.461(3), O4 B2 1.360(3), O5 B2 1.363(3), O6 B2 1.364(3) O4 C33 1.392(3), N1 C1 1.364(3), N2 C1 1.357(3), O4 B2 O5 119.8(2), O4 B2 O6 121.1(2), O5 B2 O6 119.0(2), O2 B1 O3 109.7(2), O2 B1 O1 114.1(2), O3 B1 O1 107.4(2).

Recently, Selander and co-workers disclosed the Lewis acid catalysed annulation of various nitrones with oxiranes, aziridines and thiranes, respectively [10a]. After an extensive screening, AlCl<sub>3</sub> was found to be the most active catalyst in selectively producing trans-2-methyl-3,6-diphenyl-1,4,2-dioxazine (trans-**11**) via reaction of PhCH=N(O)Me with styrene oxide (Scheme 4). The comparatively high Lewis acidities of (*R*)-**1**, (*R,R*)-**2** and (*R,R,R*)-**5** combined with their chirality prompted

us to investigate their efficacy as Lewis acid catalysts in the reaction of PhCH=N(O)Me with styrene oxide.

In a typical experiment, one equivalent of styrene oxide was added to a toluene solution of one equivalent of PhCH=N(O)Me and 5 mol% of catalyst at room temperature, the results are shown Table 1 and Figure 5.



**Scheme 4.** Lewis acid catalysed annulation of styrene oxide and PhCH=N(O)Me to trans-**11**.

Of the catalyst systems tested, (*R*)-**1** proved the most active catalyst with quantitative substrate conversion after 2 hours. The reaction proceeded with high regio- and diastereoselectivity to generate trans-**11** in ca. 90% yield (85–90% isolated yields, 1 mmol scale) after 2 hours [17]. For comparison, Selanders catalyst, AlCl<sub>3</sub>, quantitatively converted *rac*-styrene oxide after 7 hours (40°C) in anhydrous acetonitrile under argon atmosphere [10a].

Employing (*R*)- and (*S*)-styrene oxide as substrates, gave the enantiopure 1,4,2-dioxazines (*R,R*)-**11** or (*S,S*)-**11**, respectively, in high yields after 2 hours. (*R,R*)-**2** showed similar selectivities but with somewhat lower yield. The catalytic activities of (*R,R,R*)-**5** and (*R*)-**7** were significantly lower, with formation of racemic mixtures of trans-**11** in only 48 and 37% yields, respectively, after 10 hours (Figure 5). Prolonging the reaction time or increasing temperatures did not improve yields and conversion suggesting catalysts deactivation or degradation.

**Table 1.** Lewis acid catalysed formation of trans-**11**.<sup>a</sup>

Entry	catalyst	Styrene oxide	Time	Temp.	Conv.	ee
	5 mol%		[hr.]	[°C]	[%]	[%]
1	( <i>R</i> )-BINOL	<i>rac</i>	24	25	0	-
2	( <i>R</i> )- <b>1</b>	<i>rac</i>	2	25	99	6
3	( <i>R</i> )- <b>1</b>	<i>S</i>	2	25	99	99
4	( <i>R</i> )- <b>1</b>	<i>R</i>	2	25	99	98
5	( <i>R,R</i> )- <b>2</b>	<i>rac</i>	2	25	85	0
6	( <i>R,R,R</i> )- <b>5</b>	<i>rac</i>	2	25	45	-
7	( <i>R,R,R</i> )- <b>5</b>	<i>rac</i>	24	25	61	0
8	( <i>R</i> )- <b>7</b>	<i>rac</i>	2	25	31	-
9	( <i>R</i> )- <b>7</b>	<i>rac</i>	24	25	53	0

<sup>a</sup> Conditions: 0.5 mL toluene, 0.17 mmol styrene oxide, 0.17 mmol nitronone,  $8.5 \times 10^{-3}$  mmol catalyst and 0.17 mmol 1,3,5-trimethoxybenzene as internal standard (conversions determined by <sup>1</sup>H NMR spectroscopy).

It is worthwhile noting that the enantiomeric excess with catalyst (*R*)-**1** and *rac*-styrene oxide was only ca 6% (Table 1, entry 2). Running the experiment with one equivalent of nitronone and two equivalents of *rac*-styrene oxide increased the enantiomeric excess only slightly to ca. 9%. To gain more insights, the kinetic profiles for (*R*)-, (*S*)- and *rac*-styrene oxide as substrates with 5 mol% of (*R*)-**1** were obtained (Figure S48).

Consistent with our expectation based on the poor enantiomeric excess, the rates for all three styrene oxide substrates were found to be very similar.

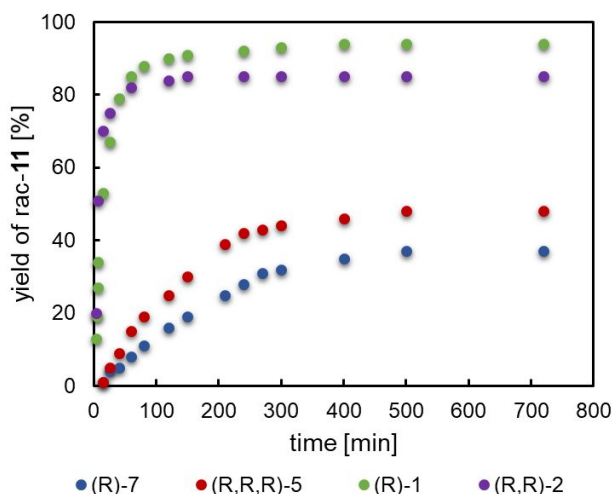


**Figure 5.** Evolution of yields in the Lewis acid catalysed annulation of *rac*-styrene oxide to *trans*-**11** with (*R*)-**1**, (*R,R*)-**2**, (*R*)-**7** and (*R,R,R*)-**5** as the catalysts. Conditions: 0.5 mL C<sub>6</sub>D<sub>6</sub>, 0.15 mmol styrene oxide, 0.15 mmol nitron, 7.5 × 10<sup>-3</sup> mmol catalyst and 0.15 mmol 1,3,5-trimethoxybenzene as internal standard (product yields determined by <sup>1</sup>H NMR spectroscopy).

To gain some mechanistic insights, stoichiometric experiments with catalysts (*R*)-**1** and (*R,R*)-**2** and substrates styrene oxide and PhCH=N(O)Me were performed under strictly anhydrous conditions in J-Young NMR tubes with C<sub>6</sub>D<sub>6</sub> as solvent (see SI for further information). The results show that PhCH=N(O)Me readily replaces THF in (*R*)-**1** to give the nitron adduct (*R*)-**4**, the latter is also formed upon adding two equiv. of nitron to (*R,R*)-**2** (see also Scheme 2). Subsequent addition of styrene oxide resulted in both cases in the formation of *trans*-**11** as the major product. However, when styrene oxide was added first to (*R*)-**1** or (*R,R*)-**2**, substantial oligo- and polymerization of styrene oxide was noted. Note also that *trans*-**11** did not form any stable adduct, neither with (*R*)-**1** nor with (*R,R*)-**2** as confirmed by <sup>1</sup>H NMR spectroscopy. We hypothesize that coordination of styrene oxide to the central boron of the catalyst caused by a replacement of the nitron in its adduct (*R*)-**4** is key to the catalytic process. The resulting Lewis acid-base interactions between styrene oxide and the catalyst activate the epoxide C-O bond and facilitate its ring opening via nucleophilic attack of the nitron with inversion in configuration at carbon. Upon recyclization, product *trans*-**11** is quickly liberated from the catalyst.

## Conclusions

We have synthesized and structurally characterized some BINOL-supported aryl boronates and boronium salts. Their high Lewis acidities combined with chirality makes them potentially attractive Lewis acid catalysts for organic transformation, which we demonstrated for the Lewis acid catalysed regio- and diastereoselective annulation of styrene oxide with nitron,

PhCH=NMe(O). Although this catalytic reaction proceeded with high regio- and diastereoselectivity to give *trans*-2-methyl-3,6-diphenyl-1,4,2-dioxazine in excellent isolated yields, the enantioselectivity of the process with 9% enantiomeric excess was lacking. To unfold their true potential in enantioselective catalysis, boronates electronically similar to (*R*)-**1** but supported by sterically more demanding BINOL ligands will have to be developed.

## Conflicts of interest

There are no conflicts to declare.

## Acknowledgements

This research was supported by the U.S. Department of Energy, Office of Science, Office of Basic Energy Sciences, Catalysis Science Program, under Award DE-SC0019094. Parts were also funded by the NSF (grant no. 1407681; Project SusChEM: IUPAC) as part of the IUPAC International Funding Call on “Novel Molecular and Supramolecular Theory and Synthesis Approaches for Sustainable Catalysis”

## Notes and references

- 1 a) D. Kaufmann, and R. Boese, *Angew. Chem.* 1990, **102**, 568-9; b) G. Hu, A. K. Gupta, L. Huang, W. Zhao, X. Yin, W. E. G. Osminski, R. H. Huang, W. D. Wulff, J. A. Izzo, and M. J. Veticatt, *J. Am. Chem. Soc.* 2017, **139**, 10267-10285.
- 2 a) R. R. Groleau, T. D. James, and S. D. Bull, *Coord. Chem. Rev.* 2021, **428**, 213599; b) D. A. Tickell, M. F. Mahon, S. D. Bull, and T. D. James, *Org. Lett.* 2013, **15**, 860-863; c) G. Mirri, S. D. Bull, P. N. Horton, T. D. James, L. Male, and J. H. R. Tucker, *Am. Chem. Soc.* 2010, **132**, 8903-8905; d) E. Galbraith, A. M. Kelly, J. S. Fossey, G. Kociok-Koehn, M. G. Davidson, S. D. Bull, and T. D. James, *New J. Chem.* 2009, **33**, 181-185.
- 3 a) D. S. Barnett, P. N. Moquist, and S. E. Schaus, *Angew. Chem., Int. Ed.* 2009, **48**, 8679-8682; b) T. R. Wu, and J. M. Chong, *J. Am. Chem. Soc.* 2006, **128**, 9646-9647; c) T. R. Wu, L. Shen, and J. M. Chong, *Org. Lett.* 2004, **6**, 2701-2704; d) J. M. Chong, L. Shen, and N. J. Taylor, *J. Am. Chem. Soc.* 2000, **122**, 1822-1823; e) K. Ishihara, S. Kondo, H. Kurihara, H. Yamamoto, S. Ohashi, and S. Inagaki, *J. Org. Chem.* 1997, **62**, 3026-3027; f) K. Ishihara, H. Kurihara, and H. Yamamoto, *J. Am. Chem. Soc.* 1996, **118**, 3049-50.
- 4 R. Alam, T. Vollgraff, L. Eriksson, and K. J. Szabo, *J. Am. Chem. Soc.* 2015, **137**, 11262-11265.
- 5 a) M. Hatano, T. Mizuno, A. Izumiseki, R. Usami, T. Asai, M. Akakura, and K. Ishihara, *Angew. Chem., Int. Ed.* 2011, **50**, 12189-12192; b) M. Hatano, T. Sakamoto, T. Mizuno, Y. Goto, and K. Ishihara, *J. Am. Chem. Soc.* 2018, **140**, 16253-16263.
- 6 a) S. Thormeier, B. Carboni, and D. E. Kaufmann, *J. Organomet. Chem.* 2002, **657**, 136-145; b) W. Clegg, T. R. F. Johann, T. B. Marder, N. C. Norman, A. G. Orpen, T. M. Peakman, M. J. Quayle, C. R. Rice, and A. J. Scott, *J. Chem. Soc., Dalton Trans.* 1998, 1431-1438.
- 7 a) M. Mewald, R. Froehlich, and M. Oestreich, *Chem. Eur. J.* 2011, **17**, 9406-9414; b) J. Hermeke, M. Mewald, E. Irran, and M. Oestreich, *Organometallics* 2014, **33**, 5097-5100.
- 8 a) L. Suesse, J. Hermeke, and M. Oestreich, *J. Am. Chem. Soc.* 2016, **138**, 6940-6943; b) L. Suesse, M. Vogler, M. Mewald, B. Kemper, E. Irran, and M. Oestreich, *Angew. Chem., Int. Ed.*

- 2018, **57**, 11441-11444; c) M. Mewald, and M. Oestreich, *Chem. Eur. J.* 2012, **18**, 14079-14084.
- 9 For boron cations in catalysis: a) W. E. Piers, S. C. Bourke, and K. D. Conroy, *Angew. Chem. Int. Ed.* 2005, **44**, 5016-5036; b) A. Prokofjevs, J. W. Kampf, and E. Vedejs, *Angew. Chem. Int. Ed.* 2011, **50**, 2098-2101; c) T. S. De Vries, A. Prokofjevs, and E. Vedejs, *Chem. Rev.* 2012, **112**, 4246-4282.
- 10 a) S. R. Pathipati, V. Singh, L. Eriksson, and N. Selander, *Org. Lett.* **2015**, **17**, 4506-4509; b) I. A. Wani, M. Sayyad, and M. K. Ghorai, *Chem. Commun.* **2017**, **53**, 4386-4389.
- 11 a) U. Mayer, V. Gutmann, and W. Gerger, *Monatsh. Chem.* **1975**, **106**, 1235-1257; b) M. A. Beckett, G. C. Strickland, J. R. Holland, and K. S. Varma, *Polymer* **1996**, **37**, 4629-4631.
- 12 S. Mummadi, D. Kenefake, R. Diaz, D. K. Unruh, and C. Krempner, *Inorg. Chem.* 2017, **56**, 10748-10759.
- 13 C. P. Manankandayalage, D. K. Unruh, and C. Krempner, *Dalton Trans.* 2020, **49**, 4834-4842.
- 14 G. J. P. Britovsek, J. Ugoletti, and A. J. P. White, *Organometallics* 2005, **24**, 1685-1691.
- 15 M. Eck, S. Würtemberger-Pietsch, A. Eichhorn, J. H. J. Berthel, R. Bertermann, U. S. D. Paul, H. Schneider, A. Friedrich, C. Kleeberg, U. Radius, and T. B. Marder, *Dalton Trans.*, 2017, **46**, 3661-3680.
- 16 S. Würtemberger-Pietsch, H. Schneider, T. B. Marder, and U. Radius, *Chem. Eur. J.*, 2016, **22**, 13032-13036.